JOURNAL OF GEOPHYSICAL RESEARCH, VOL. 106, NO. A7, PAGES 13,165–13,178, JULY 1, 2001

Substorm dependence of chorus amplitudes: Implications for the acceleration of electrons to relativistic energies

Nigel P. Meredith

Mullard Space Science Laboratory, University College London, Holmbury St Mary, Surrey, United Kingdom

Richard B. Horne

British Antarctic Survey, Natural Environment Research Council, Cambridge, United Kingdom

Roger R. Anderson

Department of Physics and Astronomy, University of Iowa, Iowa City, Iowa

Abstract. Intense interest currently exists in determining the roles played by various wave-particle interactions in the acceleration of electrons to relativistic energies during/following geomagnetic storms. Here we present a survey of wave data from the CRRES Plasma Wave Experiment for lower band (0.1-0.5f_{ce}) and upper band (0.5-1.0f_{ce}) chorus, f_{ce} being the electron gyrofrequency, to assess whether these waves could play an important role in the acceleration of a seed population of electrons to relativistic energies during and following geomagnetic storms. Outside of the plasmapause the chorus emissions are largely substorm-dependent, and all chorus emissions are enhanced when substorm activity is enhanced. The equatorial chorus ($| \lambda_m | < 15^o$) is strongest in the lower band during active conditions ($AE > 300$ nT) with average amplitudes typically >0.5 mV m^{-1} predominantly in the region $3 < L < 7$, between 2300 and 1300 magnetic local time (MLT). This is consistent with electron injection near midnight and subsequent drift around dawn to the dayside. The high-latitude chorus ($| \lambda_m | > 15^o$) is strongest in the lower band during active conditions, with average amplitudes typically >0.5 mV m^{-1} in the region $3 < L < 7$ over a range of local times on the dayside, principally in the range 0600-1500 MLT, consistent with wave generation in the horns of the magnetosphere. An inner population of weak, substorm-independent emissions with average amplitudes generally <0.2 mV m^{-1} are seen in both bands largely inside $L = 4$ on the nightside during quiet ($AE < 100$ nT) and moderate (100 nT $< AE <$ 300 nT) conditions. These emissions lie inside the plasmapause and are attributed to signals from lightning and ground-based VLF transmitters. We conclude that the significant increases in chorus amplitudes seen outside of the plasmapause during substorms support the theory of electron acceleration by whistler mode chorus in that region. The results suggest that electron acceleration by whistle mode chorus during/following geomagnetic storms can only be effective when there are periods of prolonged substorm activity following the main phase of the geomagnetic storm.

1. Introduction

The flux of relativistic electrons (>1 MeV) in the outer radiation belt ($L > 3.5$) varies substantially during geomagnetic storms. Typically, the relativistic electron flux may fall by up to 2 or 3 orders of magnitude over a period of several hours at the beginning of the main phase. Subsequently, the flux may rise to peak levels 10-100 times the prestorm values over a period of 2-3 days during the recovery stage. There are several mechanisms which contribute to the initial flux decrease, including adiabatic effects associated with the decrease of Dst, loss due to precipitation to the atmosphere,

Paper number 2000JA900156.
0148-0227/01/2000JA900156$09.00

and outward drift and loss via scattering at the magnetopause [*Li et al.*, 1997a]. Observations suggest that the subsequent flux increase over longer timescales during the recovery phase cannot be explained by adiabatic effects alone [*Li et al.*, 1997a]. Furthermore, the electron phase space density in the solar wind is too low to supply the outer radiation belt directly [*Li et al.*, 1997b]. These results imply that the increases in the relativistic electron flux are caused by acceleration processes within the magnetosphere itself, although the exact nature of these processes remains elusive. A number of acceleration mechanisms have been proposed, including radial diffusion [*Schulz and Lanzerotti*, 1974], global recirculation processes [*Fujimoto and Nishida*, 1990], ULF waves [*Rostoker et al.*, 1998; *Liu et al.*, 1999; *Hudson et al.*, 2000], wave-particle interactions [*Li et al.*, 1997a; *Horne and Thorne*, 1998; *Summers et al.*, 1998; *Summers and Ma*, 2000], and acceleration mechanisms operating in the outer polar cusp region [*Sheldon et al.*, 1998]. The determination of the mechanism(s) responsible for the acceleration is a major area of current research, and here we consider the role of wave-particle interactions.

Enhanced storm time convection electric fields can provide a seed population of electrons with energies of the order of a few hundred keV. Wave-particle interactions then provide a mechanism for accelerating this seed population to relativistic values. *Horne and Thorne* [1998] identified several wave modes which could accelerate electrons to MeV energies via Doppler-shifted cyclotron resonance. In particular, they showed that whistler mode waves are able to resonate with electrons from 100 keV to several MeV, showing that these waves could, in principle, accelerate electrons in the seed population up to MeV energies. In a related paper, *Summers et al.* [1998] considered the diffusion curves for resonant interactions with parallel propagating whistler mode waves and showed that significant energization can occur during resonant interactions with these waves. These studies suggest that whistler mode waves could be very important for both electron loss [e.g., *Lyons et al.*, 1972] and acceleration during storm times.

Both chorus and hiss are whistler mode emissions observed inside the magnetosphere. Hiss is usually observed inside the plasmapause at frequencies between 0.1 and 3 kHz and is believed to be responsible for electron loss and the formation of the slot region ($L \sim 2.5$) between the inner and outer radiation belts [*Thorne and Kennel*, 1971; *Lyons et al.*, 1972]. Chorus, on the other hand, is observed predominantly outside the plasmapause in the frequency range 0.1-0.8f_{ce} [*Tsurutani and Smith*, 1977; *Koons and Roeder*, 1990]. *Summers et al.* [1998] showed that energy diffusion over the important energy range 100 keV < E < 1 MeV becomes more significant for smaller values of the ratio of the electron plasma frequency, f_{pe}, to the electron gyrofrequency, f_{ce}, suggesting that chorus emissions outside the plasmapause may be more important for electron energization than hiss.

Chorus emissions are often observed in two distinct bands: one above and one below $0.5f_{ce}$ [*Tsurutani and Smith*, 1974]. The width of the gap between the bands is highly variable, sometimes reaching $0.2f_{ce}$ and sometimes disappearing altogether [*Koons and Roeder*, 1990]. Various mechanisms have been invoked to explain this gap, including a Landau damping mechanism first proposed by *Tsurutani and Smith* [1974] and a two-source model put forward by *Maeda et al.* [1976].

Statistical surveys show that chorus occurs principally in two magnetic latitude regions, one near the equator ($|\lambda_m| < 15^o$) and one at higher latitudes ($|\lambda_m| > 15^o$) [*Tsurutani and Smith*, 1977]. Equatorial chorus is substorm related [*Tsurutani and Smith*, 1974, 1977; *Meredith et al.*, 2000] and occurs principally in the region from 0000 to 1500 magnetic local time (MLT), peaking in the dawn to noon quadrant (see, for example, *Tsurutani and Smith* [1977] and *Koons and Roeder* [1990]). High-latitude chorus is not strongly dependent on substorm activity and is often observed during magnetically quiet periods [*Tsurutani and Smith*, 1977]. High-latitude chorus occurs primarily on the dayside and often within 1-2 R_E of the magnetopause.

Statistical surveys of chorus emissions have concentrated on the morphology and frequency of occurrence [e.g., *Tsurutani and Smith*, 1977; *Koons and Roeder*, 1990]. Maps of the average whistler mode wave amplitude as a function of frequency and local time have been produced [*Parrot and Gaye*, 1994], but they are restricted to geostationary orbit. There has been very little work to quantify the spatial dependence of the chorus amplitudes as a function of magnetic activity in the radiation belts. Amplitude information is essential for calculations of pitch angle and energy diffusion rates and hence for quantifying the contribution of whistler mode chorus for electron energization. Here we present a quantitative survey of whistler mode chorus amplitudes using data from the Combined Release and Radiation Effects Satellite (CRRES) to determine the spatial dependence of chorus amplitudes as a function of magnetic activity and to help determine where the chorus should be most effective in accelerating electrons to relativistic energies during/following geomagnetic storms.

2. Instrumentation

CRRES is particularly well suited to studies of the plasma wave environment in the radiation belts owing to the low-inclination elliptical orbit and the frequency range of the Plasma Wave Experiment. The spacecraft was launched on July 25, 1990 and operated in a highly elliptical geosynchronous transfer orbit with a perigee of 305 km, an apogee of 35,768 km and an inclination of 18°. The orbital period was approximately 10 hours, and the initial apogee was at a magnetic local time of 0800 MLT. The satellite swept through the heart of the radiation belts on average approximately 5 times per day, providing good coverage of this important region for almost 15 months.

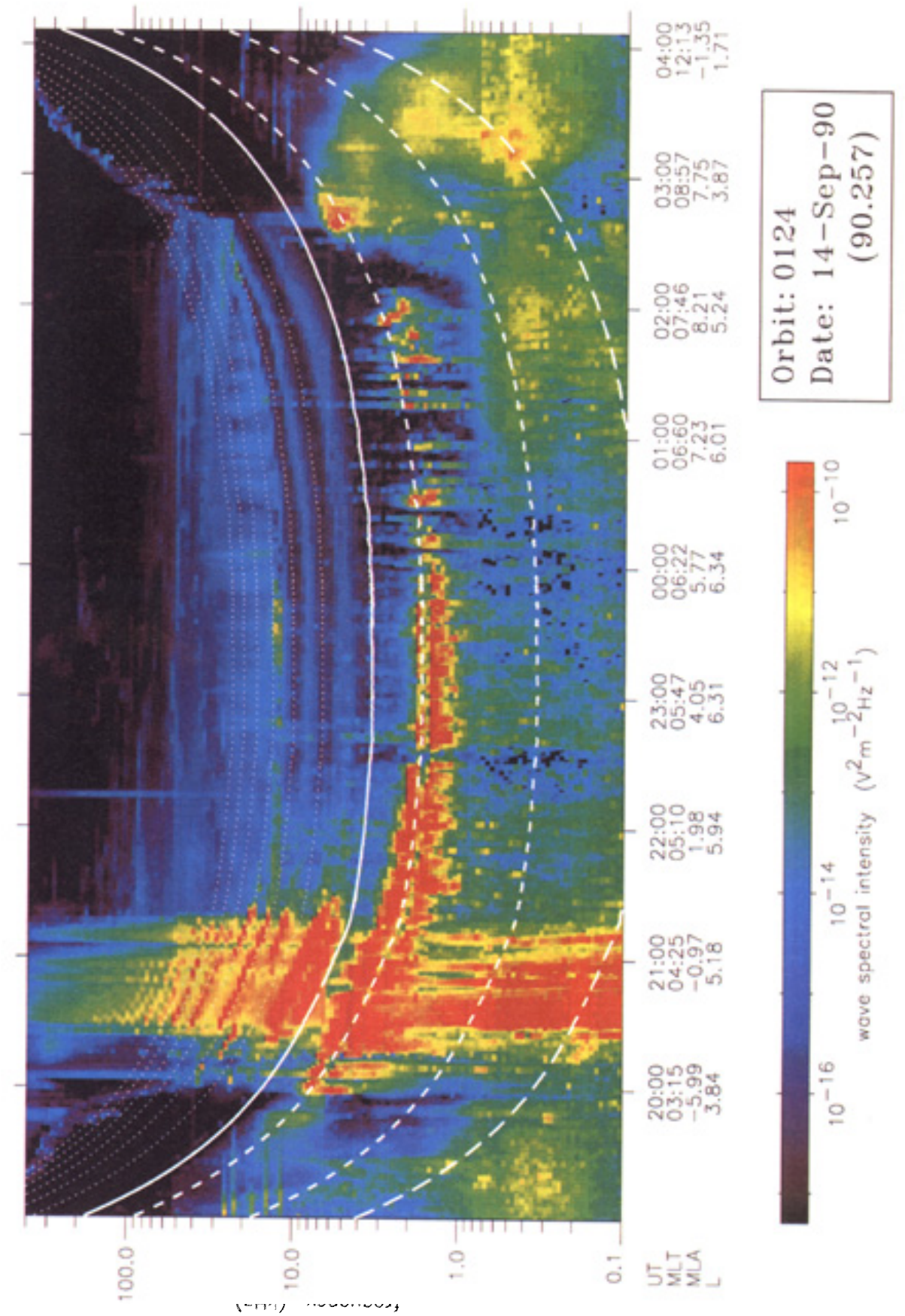

Plate 1. Survey plot of the wave spectral intensity for orbit 124 as a function of frequency and universal time. The solid white line represents the local electron gyro-frequency (f_{ce}). From bottom to top the other lines represent the local lower hybrid frequency, $0.1f_{ce}$, $0.5f_{ce}$, and the first six harmonics of f_{ce}.

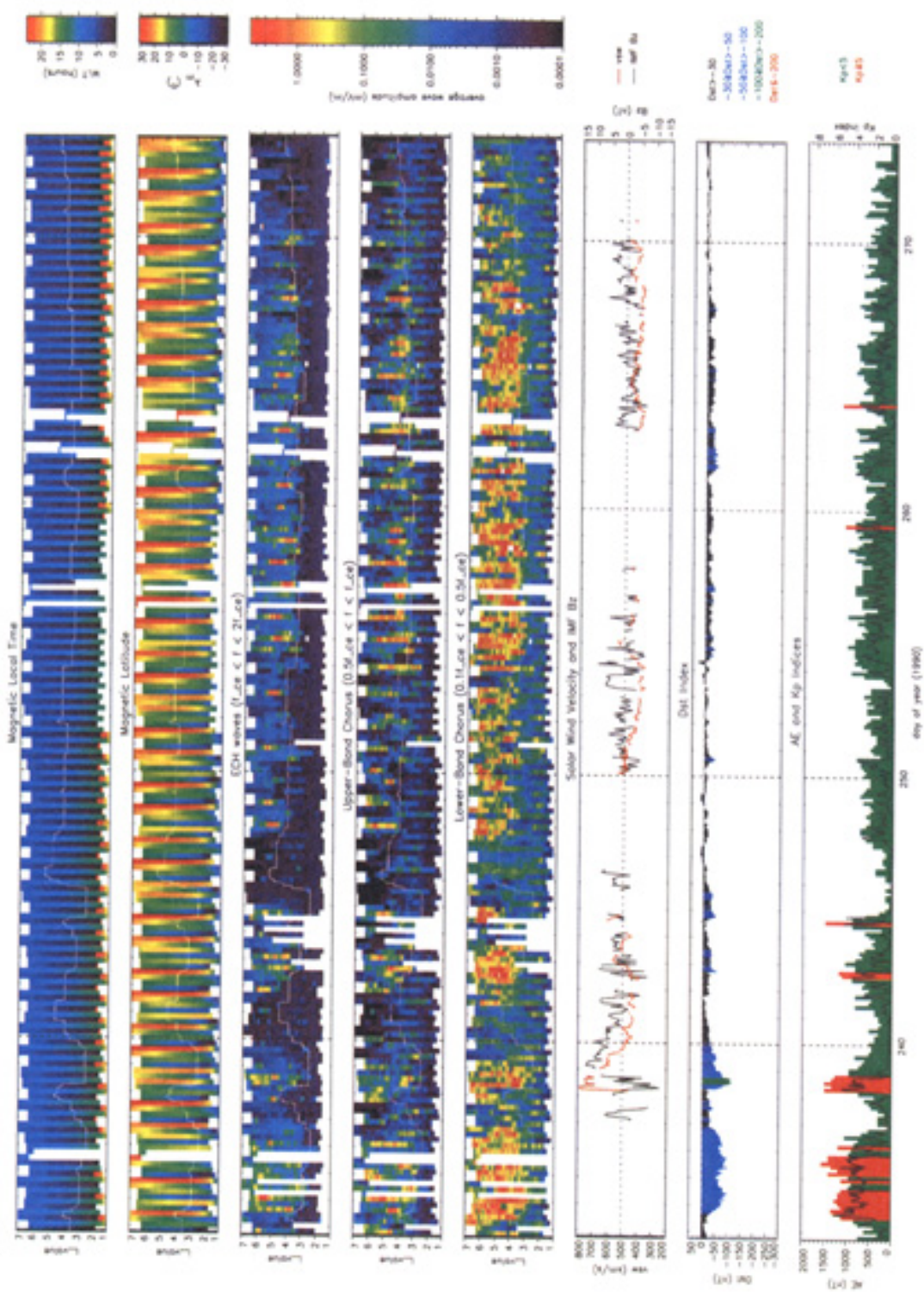

Plate 2. Rebinned data and relevant geophysical parameters for orbits 63 to 163 as a function of L and half orbit. From top to bottom, the panels show magnetic local time, magnetic latitude, wave amplitudes for ECH waves and upper band and lower band chorus, solar wind speed and interplanetary magnetic field (IMF) B_z, the color-coded Dst index, and finally, the color-coded Kp index together with a line plot of the AE index. The empirical position of the plasmapause is marked in the upper five panels as a solid white line.

The wave data used in this study were provided by the Plasma Wave Experiment on board the CRRES spacecraft. This experiment provided measurements of electric fields from 5.6 Hz to 400 kHz, using a 100 m tip-to-tip long wire antenna, and magnetic fields from 5.6 Hz to 10 kHz, using a search coil magnetometer, with a dynamic range covering a factor of at least 10^5 in amplitude [*Anderson et al.*, 1992]. The electric field detector was thus able to detect waves from below the lower hybrid resonance frequency (f_{LHR}) to well above the upper hybrid resonance frequency (f_{UHR}) for a large fraction of each orbit.

The sweep frequency receiver covered the frequency range from 100 Hz to 400 kHz in four bands with 32 logarithmically spaced steps per band, the fractional step separation, $\Delta f/f$ being about 6.7% across the entire frequency range. Band 1 (100 to 810 Hz) was sampled at one step per second with a complete cycle time of 32.768 s. Band 2 (810 Hz to 6.4 kHz) was sampled at two steps per second with a complete cycle time of 16.384 s. Band 3 (6.4 to 51.7 kHz) and band 4 (51.7 to 400 kHz) were each sampled 4 times per second, with complete cycling times of 8.192 s. The nominal bandwidths in bands 1, 2, 3, and 4 were 7 Hz, 56 Hz, 448 Hz, and 3.6 kHz, respectively.

3. Data Analysis

In order to perform a statistical analysis of the wave amplitudes, the data were initially corrected for the instrumental background response and smoothed by using a running 3-min average to take out the beating effects due to differences in the sampling and the spin rate. Spurious data points, data spikes, and periods of instrumental downtime were flagged and ignored in the subsequent statistical analyses. Twelve orbits, during which nontraditional configurations were deployed for testing purposes, were also excluded from the analyses.

Since whistler mode chorus is commonly observed in the range 0.1-0.8f_{ce} [*Koons and Roeder*, 1990] with a gap occurring at 0.5f_{ce} [*Tsurutani and Smith*, 1977], the emissions were divided into two categories which we shall refer to as lower and upper band chorus. The wave intensities were then defined by integrals of the averaged wave spectral density ($\mathrm{V^2\ m^{-2}\ Hz^{-1}}$) over the frequency range $0.1f_{\mathrm{ce}} < f < 0.5f_{\mathrm{ce}}$ (lower band chorus) and $0.5f_{\mathrm{ce}} < f < f_{\mathrm{ce}}$ (upper band chorus). The electron gyrofrequency, f_{ce}, was determined from the fluxgate magnetometer instrument on board the spacecraft [*Singer et al.*, 1992] and equals 28 Hz times the ambient field measured in nanoteslas. The corresponding wave amplitudes were obtained by taking the square root of the appropriate integrated spectral densities. The background noise levels for the derived wave amplitudes are of the order of 5×10^{-4} mV m^{-1}. The amplitudes were then rebinned as a function of half orbit (outbound or inbound) and L in steps of $0.1L$ and recorded with the time in UT, magnetic latitude λ_m, magnetic local time, and time spent in each bin, at the same resolution.

The resulting data set, consisting of plasma wave measurements from 939 orbits (1878 half orbits) was subsequently analyzed to determine the behavior of the chorus amplitudes as a function of one or two of the spatial parameters (L, MLT, λ_m) and magnetic activity.

4. Initial Results

An example of enhanced chorus emissions occurring during a period of substorm activity is shown in Plate 1. This spectrogram shows the corrected and smoothed wave data for orbit 124. Here the wave spectral intensity is plotted against UT time for the entire orbit beginning at perigee at 1900:03 UT on September 14, 1990, and ending at the next perigee at 0406:40 UT on September 15, 1990. The magnetic local time, magnetic latitude and L value are also given at hourly intervals. The solid white line shows the value of f_{ce}, determined from the measured ambient magnetic field. The long-dashed line represents the local lower hybrid resonance frequency f_{LHR}, the dashed lines represent $0.1f_{\mathrm{ce}}$ and $0.5f_{\mathrm{ce}}$, and the dotted lines represent harmonics of the electron gyrofrequency Nf_{ce}. The enhanced emissions at approximately 13 kHz at 2300 UT correspond to oscillations at the local upper hybrid resonance frequency f_{UHR}. When clearly visible, these emissions provide an estimate of the local electron number density.

Enhanced upper and lower band chorus intensities are seen as the spacecraft exits the plasmapause around 2000 UT. These emissions show a gap or drop in intensity at approximately $0.5f_{\mathrm{ce}}$ and are an example of double-banded chorus reported by previous workers [*Tsurutani et al.*, 1974]. An example of some weak chorus activity inside the plasmapause may be seen between 1920 and 2000 UT at frequencies near 10 kHz. These emissions could be the result of magnetospherically reflected whistlers [e.g., *Thorne and Horne*, 1994] or could be due to chorus waves leaking into the plasmasphere [*Anderson*, 1994].

Enhanced electron cyclotron harmonic (ECH) waves are seen between 2025 UT and 2115 UT. These waves, which propagate between the harmonics of the electron gyrofrequency, are substorm-dependent and tend to be confined to the equatorial region [*Meredith et al.*, 2000].

Plasmaspheric hiss can be identified by the emissions below about 3 kHz before 2000 UT and after 0300 UT. They occur primarily inside the high-density regions. Note that these emissions appear to be unrelated to any of the characteristic frequencies of the plasma, with the possible exception of a burst of higher-frequency emissions at about 500 Hz near 0315 UT which may be related to the lower hybrid resonance frequency. The horizontal lines between 10 and 25 kHz before 2000 UT and after 0300 UT are from ground-based VLF transmitters used for navigation and communication with submarines.

A plot of the rebinned wave amplitudes for orbits 63 to 163 is shown in Plate 2. From top to bottom the

panels show the magnetic local time, the magnetic latitude, wave amplitudes for ECH waves, upper band and lower band chorus, solar wind speed and IMF B_z data from IMP 8, the color-coded Dst index, and finally, the color-coded Kp index together with a line plot of the AE index. The approximate position of the plasmapause, L_p, given by the expression

$$L_p = 5.6 - 0.46Kp^*, \quad (1)$$

where Kp^* is the maximum value of Kp in the previous 24 hours [*Carpenter and Anderson*, 1992], is marked on the amplitude and location plots as a thin white line. Using this empirical model, enhanced chorus emissions lie mainly outside the plasmapause. Moreover, as the plasmapause moves to smaller L during magnetically active periods, the inner edge of the chorus emissions also moves to smaller L and follows the plasmapause position very closely.

Inspection of this plot shows that the chorus emissions are best correlated with the AE index, a result which is consistent with previous observations that the chorus activity is substorm-dependent [*Tsurutani and Smith*, 1974, 1977; *Meredith et al.*, 2000]. We therefore choose to measure the magnetic activity with the AE index, defining the conditions as being quiet ($AE < 100$ nT), moderate ($100 < AE < 300$ nT), or active ($AE > 300$ nT) depending on the value of AE at the time of the observation.

5. Substorm Dependence of Chorus Amplitudes as a Function of L and Magnetic Local Time

Tsurutani and Smith [1977] showed that the chorus emissions could be divided into two categories depending on magnetic latitude. The same scheme and notation are adopted here with equatorial and high-latitude chorus being defined as chorus observed within and beyond 15° of the magnetic equator, respectively. We begin by studying the substorm dependence of the chorus amplitudes in these regions as a function of L and magnetic local time.

5.1. Equatorial Chorus

The equatorial lower band chorus amplitudes are shown as a function of L, MLT and substorm activity in the lower panels of Plate 3. Here the average amplitudes are plotted in the large panels, and the corresponding sampling distributions are in the small panels. During quiet conditions the wave amplitudes are generally less than 0.1 mV m^{-1} over the entire region. Elevated wave amplitudes in the range $0.1 < E_0 < 0.5$ mV m^{-1} are seen during moderate conditions mainly in the region $L > 4$ between 0000 and 0800 MLT. The waves are most enhanced and cover the largest region of geospace during active conditions with amplitudes typically >0.5 mV m^{-1} predominantly in the region $L > 3$ from 2300 to 1300 MLT. The inner boundary lies outside of the plasmapause and moves to smaller L with the plasmapause during active conditions. These results show that outside of the plasmapause the lower band equatorial chorus is largely substorm-dependent. There is also evidence of an inner population of weak emissions with average amplitudes of the order of 0.2 mV m^{-1} in the region $2 < L < 3$ extending from approximately 1900 to 0900 MLT. These emissions lie in the high-density region inside the plasmapause and are not substorm related, since the change in amplitude with AE is very small.

The equatorial upper band chorus amplitudes are shown in a similar format in the upper panels of Plate 3. The amplitudes are generally lower than the corresponding lower band chorus. The average amplitudes are generally less than 0.05 mV m^{-1} during quiet conditions. Elevated wave amplitudes in the range $0.05 < E_0 < 0.2$ mV m^{-1} are encountered during moderate conditions mainly in the region $L > 4$ from 0000 to 0700 MLT. The wave amplitudes are most enhanced during active conditions with amplitudes >0.1 mV m^{-1} predominantly in the region $L > 3$ between 2300 and 1300 MLT. These results show that outside of the plasmapause the upper band equatorial chorus is also largely substorm-dependent. There is also evidence for a weak inner population inside $L = 4$, with amplitudes in the range $0.01 < E_0 < 0.05$ mV m^{-1} largely in the region $3 < L < 4$ extending from approximately 1900 to 0900 MLT for weak to moderate activity. This population most likely lies inside the high-density plasmapause region for low and moderate levels of magnetic activity and is not substorm related. For stronger activity, the waves between $3 < L < 4$ are enhanced in the postmidnight, early morning sector and are most likely outside the plasmapause as the plasmapause moves to lower L during active conditions.

5.2. High-Latitude Chorus

The high-latitude lower band chorus is shown as a function of L, MLT, and substorm activity in the lower panels of Plate 4. As before, the amplitudes in the region outside the plasmapause are largely substorm-dependent. However, the spatial dependence of the population is clearly different from equatorial lower band chorus with peak amplitudes typically >0.5 mV m^{-1} occurring in the region $L > 3$ during active conditions on the dayside, predominantly in the range 0600-1500 MLT. There is also evidence of a weak inner population with amplitudes of the order of 0.2 mV m^{-1} lying mainly inside the plasmapause between 1900 and 0600 MLT. These emissions are observed during quiet and moderate conditions and are largely substorm-independent.

The high-latitude upper band chorus is shown in a similar format in the upper panels of Plate 4. The average amplitudes outside the plasmapause are largely

substorm-dependent, peaking during active conditions with amplitudes typically >0.01 mV m^{-1} between 1900 and 1300 MLT with evidence for a reduction in amplitude around dawn. These peak amplitudes are over an order of magnitude lower than the corresponding high-latitude lower band chorus emissions. There is also a weak inner population with amplitudes of the order of 0.01 mV m^{-1} occurring predominantly inside the plasmapause and extending from 1800 to 0600 MLT which is largely substorm-independent.

6. Substorm Dependence of Chorus Amplitudes as a Function of L and Magnetic Latitude

The statistical analysis has shown that the average chorus amplitudes may be conveniently categorized as a function of L, magnetic local time, magnetic latitude, and substorm activity. We now take a detailed look at the behavior of the chorus amplitudes as a function of L and magnetic latitude by dividing the local time coverage into two sectors, 2100-0600 MLT and 0600-1500 MLT, corresponding to the two regions where the waves are enhanced during substorm activity. There is very little evidence for enhanced waves in the region 1500-2100 MLT and so this region is not discussed further.

6.1. Nightside to Dawn Sector 2100-0600 MLT

The lower band chorus amplitudes for this sector are shown as a function of the radial distance from the center of the Earth projected onto the plane of the magnetic equator, x, GSM z, and substorm activity in the lower panels of Plate 5. Dipole field lines and lines of constant magnetic latitude are included on the plot to help visualize the behavior of the wave amplitudes as a function of L and magnetic latitude. As before, the average amplitudes are plotted in the large panels and the corresponding sampling distributions in the small panels. The substorm-dependent emissions outside the plasmapause are largely confined to the magnetic equatorial region, peaking with amplitudes typically >0.5 mV m^{-1} over the latitude range $|\lambda_m| < 15°$. In contrast, the substorm-independent emissions inside the plasmapause do not exhibit any confinement with latitude.

The upper band chorus amplitudes for this sector are shown in a similar format in the upper panels of Plate 5. The substorm-dependent emissions outside the plasmapause are more tightly confined to the magnetic equatorial region, lying predominantly within ±7° of the magnetic equator. The substorm-independent emissions inside the plasmapause can be divided into two categories: an outer population that is not confined in latitude and an inner population that is confined above the magnetic equator. The outer population exhibits an inner edge that follows a line of constant $x = 2.6\ R_E$. This inner edge roughly corresponds to a line of constant magnetic field strength corresponding to $f_{ce} = 50$ kHz.

6.2. Dawn Through Dayside Sector 0600-1500 MLT

The lower band chorus amplitudes for this sector are shown as a function of the radial distance from the center of the Earth projected onto the plane of the magnetic equator, x, GSM z, and substorm activity in the lower panels of Plate 6. There are more data gaps in this sector. Nevertheless, it can be seen that the substorm-dependent lower band chorus emissions outside the plasmapause are not confined to the equatorial region but rather extend out to the largest latitudes sampled by CRRES. The substorm-independent emissions inside the plasmapause lie largely to the south of the equator.

The upper band chorus amplitudes for this sector are shown in a similar format in the upper panels of Plate 6. In this sector the substorm-dependent upper band chorus emissions outside the plasmapause are largely confined in magnetic latitude, lying approximately within 10° of the magnetic equator and do not show any evidence for stronger emissions at higher latitudes. The substorm-independent emissions inside the plasmapause exhibit a cutoff at $x = 2.6\ R_E$, but there is no evidence for an inner population inside $L = 2.6$.

7. Discussion

7.1. Substorm-Dependent Emissions and Their Possible Role in Electron Acceleration

Outside of the plasmapause the chorus emissions are largely substorm-dependent. The equatorial chorus is strongest in the lower band during active conditions over a range of L, $3 < L < 7$, in the region 2300-1300 MLT. The local time dependence of these amplitude enhancements is consistent with keV electron injection from substorms near midnight and subsequent drift around dawn to the dayside. The high-latitude chorus is observed primarily in the lower band and is strongest during active conditions in the region $3 < L < 7$ over a range of local times on the dayside, principally in the range 0600-1500 MLT. This result contrasts with that obtained previously by *Tsurutani et al.* [1977], who concluded that high-latitude chorus in the range $5 < L < 15$ is generally not substorm-dependent. We attribute the difference to the low L coverage in our study. These waves, which may be caused by wave generation in the horns of the magnetosphere [*Tsurutani et al.*, 1977], are only likely to be seen by CRRES on the smaller L during active conditions when the dayside magnetosphere is most distorted. Thus both the equatorial and high-latitude chorus emissions could contribute significantly to electron acceleration. It is now interesting to compare the wave results with the key conclusions from the particle observations.

Blake et al. [1997] showed that a high-speed solar wind stream and a leading pressure pulse can have a strong effect on the energetic electron population when the interplanetary magnetic field (IMF) turns south-

ward. More recently, *Iles et al.* [2000] have shown that the relativistic electron enhancements are correlated with the presence of high-speed solar wind streams and southward IMF during the recovery phase of the geomagnetic storm. These are conditions that lead to enhanced substorm activity, and hence our results suggest that enhanced chorus amplitudes would be seen during these intervals. Thus relativistic electron enhancements are likely to be correlated with enhanced chorus amplitudes during the recovery phase, suggesting that these waves could play a role in the acceleration of electrons to relativistic energies during/following geomagnetic storms.

Although about 90% of geomagnetic storms have been found to result in relativistic electron flux enhancements [*Reeves*, 1998], not all storms result in relativistic electron acceleration events. An interesting example of this may be seen in the survey plot in Plate 2. A moderate storm commences during day 238 with a minimum Dst of -113 nT. The solar wind speed is initially very high in the range $600 < v_{sw} < 800$ km s^{-1}, and the IMF B_z is predominantly southward. This region is characterized by enhanced lower band chorus ($0.1 < E_0 < 3.0$ mV m^{-1}) and high values of Kp ($Kp > 5$) and AE ($AE > 500$ nT). The IMF turns northward shortly after the storm main phase and remains northward for an extended period of 2 days. This period is characterised by weak lower band chorus ($0.001 < E_0 < 0.1$ mV m^{-1}), very low values of the AE index ($AE < 100$ nT), and a gradual reduction in the value of the Kp index. These results show that there is a lack of substorm activity and weak wave activity following the storm main phase in this case, suggesting that a relativistic electron enhancement would not be associated with this particular geomagnetic storm. Indeed, observations from the CRRES Magnetic Electron Spectrometer [*Vampola et al.*, 1992] confirm that this event was not associated with a relativistic electron enhancement (R. H. A. Iles, personal communication, 2000). This event suggests that the amount of substorm activity during the recovery phase of the geomagnetic storm is an important factor controlling electron acceleration on timescales of a few days and is related to the behavior of IMF B_z.

There are other periods of significant chorus activity in Plate 2 that are not associated with strong geomagnetic storms, as measured by Dst. One may expect electron acceleration to occur during these periods as well. However, there are several important differences between chorus that occurs during geomagnetic storms and chorus that is related to substorms or magnetic activity. First, during geomagnetic storms chorus can extend across a larger radial cross section of the radiation belts and to lower L. For example, in Plate 2 during the two geomagnetic storms before day 240 the plasmapause moves to lower L and chorus extends from $L \approx 2.5$ to 6. Second, since electron acceleration by chorus emissions depends on the ratio f_{pe}/f_{ce}, the location of chorus at lower L during storm times could be a factor affecting the efficiency of electron acceleration. Third, the seed population of low-energy electrons is more likely to be enhanced during geomagnetic storms than during substorms due to enhanced convection. These factors may be important for determining whether electrons are accelerated to MeV energies during geomagnetic storms, as opposed to substorms.

7.2. Substorm-Independent Emissions

The emissions inside $L = 4$ seen during weak and moderate conditions tend to lie inside the plasmapause and are largely substorm-independent. During active conditions, enhanced waves observed in the region $3 < L < 4$ are most likely outside the plasmapause as the plasmapause moves to lower L during active periods. The most likely candidates for the substorm-independent emissions are lightning-generated whistlers and VLF signals from ground-based transmitters. This suggestion is consistent with observations that these waves occur mainly on the nightside of the Earth, since signals passing through the ionosphere at VLF frequencies suffer less attenuation in the ionosphere when the ionosphere is in darkness [*Smith and Jenkins*, 1998].

Lightning-generated whistlers, in the frequency range 1-20 kHz, may penetrate through the ionosphere and propagate into the radiation belts [*Helliwell*, 1965]. VLF signals from ground-based transmitters based mainly in the Northern Hemisphere occur in two frequency bands. All the high-powered navigation transmitters operate at or below 25 kHz, and the amateur radio low-frequency band begins just below 50 kHz (D. Carpenter, personal communication, 2000).

The inner edge of the outer population of substorm-independent upper band chorus observed at $x = 2.6$ R_E is due to the gap in VLF transmitter frequencies between 25 kHz and approximately 50 kHz. When the electron gyrofrequency is 50 kHz, this frequency gap will coincide exactly with the frequency range of the upper band chorus, which explains the sudden drop in average amplitudes of the upper band chorus at $x = 2.6$ R_E where $f_{ce} = 50$ kHz. No such drop in amplitudes is seen in the substorm-independent lower band chorus, since this frequency band covers a factor of 5 in frequency.

The inner population of the substorm-independent upper band chorus emissions is observed mainly above the magnetic equator. These emissions are most likely due to VLF transmitters operating above 50 kHz, since $f_{ce}/2 > 25$ kHz in this region, above the frequency range of both lightning-generated whistlers and the high-powered navigation transmitters. Upper band chorus emissions, for which $0.5f_{ce} < f < f_{ce}$, are unguided by the field but may be guided by a plasma trough. We suggest that the confinement to the Northern Hemisphere of the inner population of upper band signals is due to the location of VLF transmitters in the Northern Hemisphere which result in unguided magnetospherically reflected signals that are confined mainly above the equator.

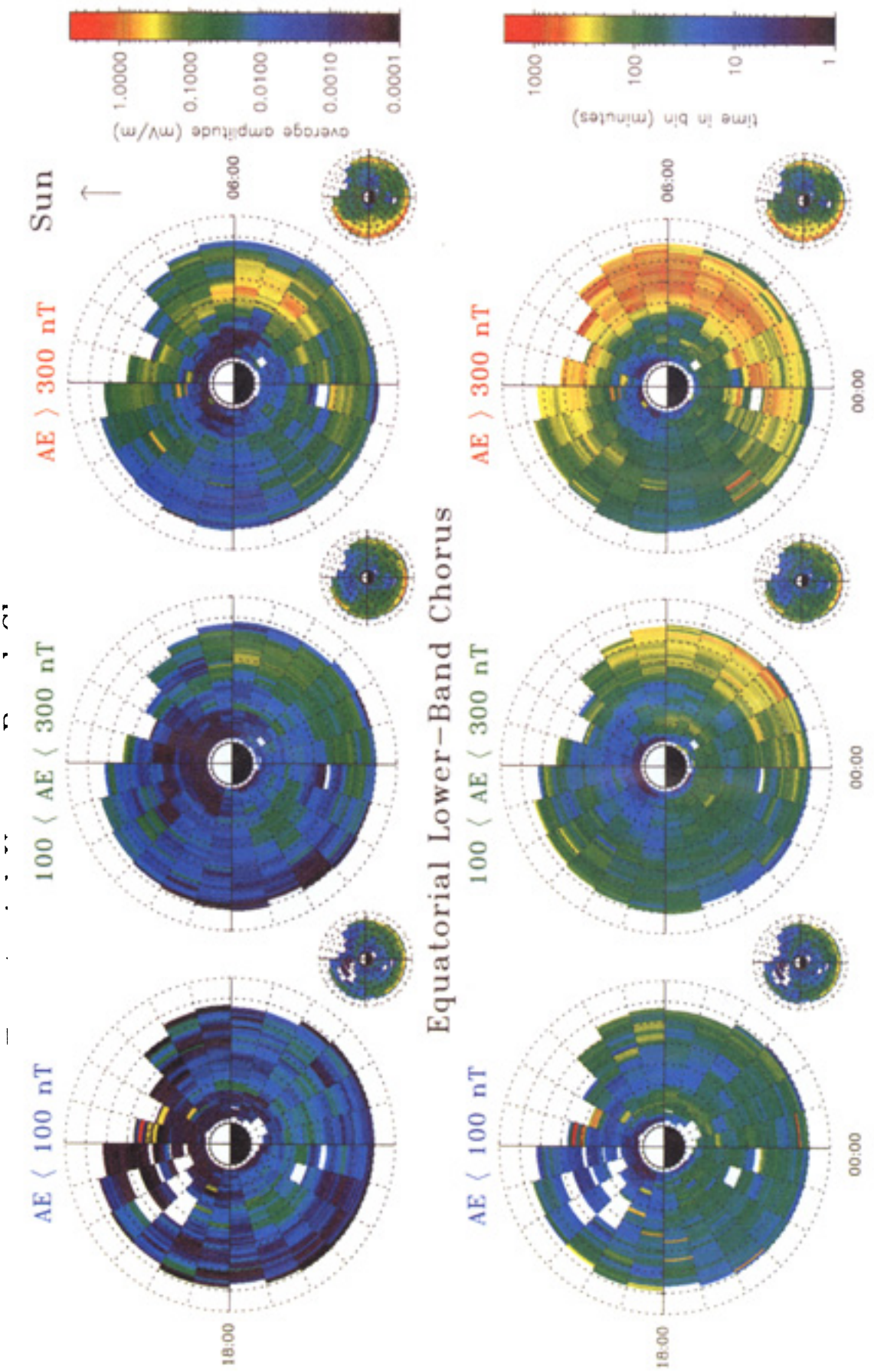

Plate 3. Substorm dependence of the average equatorial wave amplitudes for lower band chorus (lower panels) and upper band chorus (upper panels) as a function of L and MLT. The average amplitudes are shown in the large panels, together with the corresponding sampling distributions in the small panels.

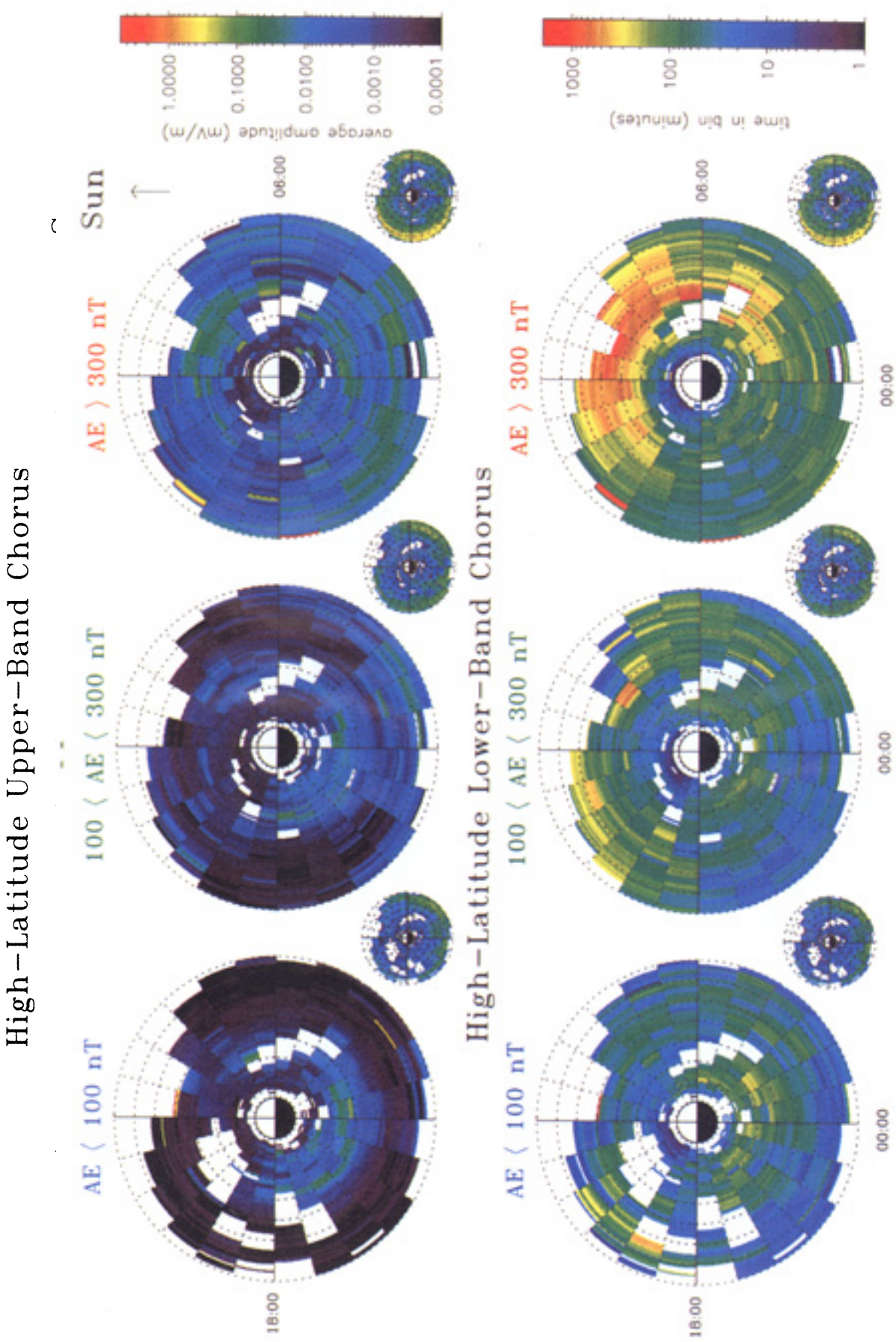

Plate 4. Substorm dependence of the average high-latitude wave amplitudes for lower band chorus (lower panels) and upper band chorus (upper panels) as a function of L and MLT. The average amplitudes are shown in the large panels, together with the corresponding sampling distributions in the small panels.

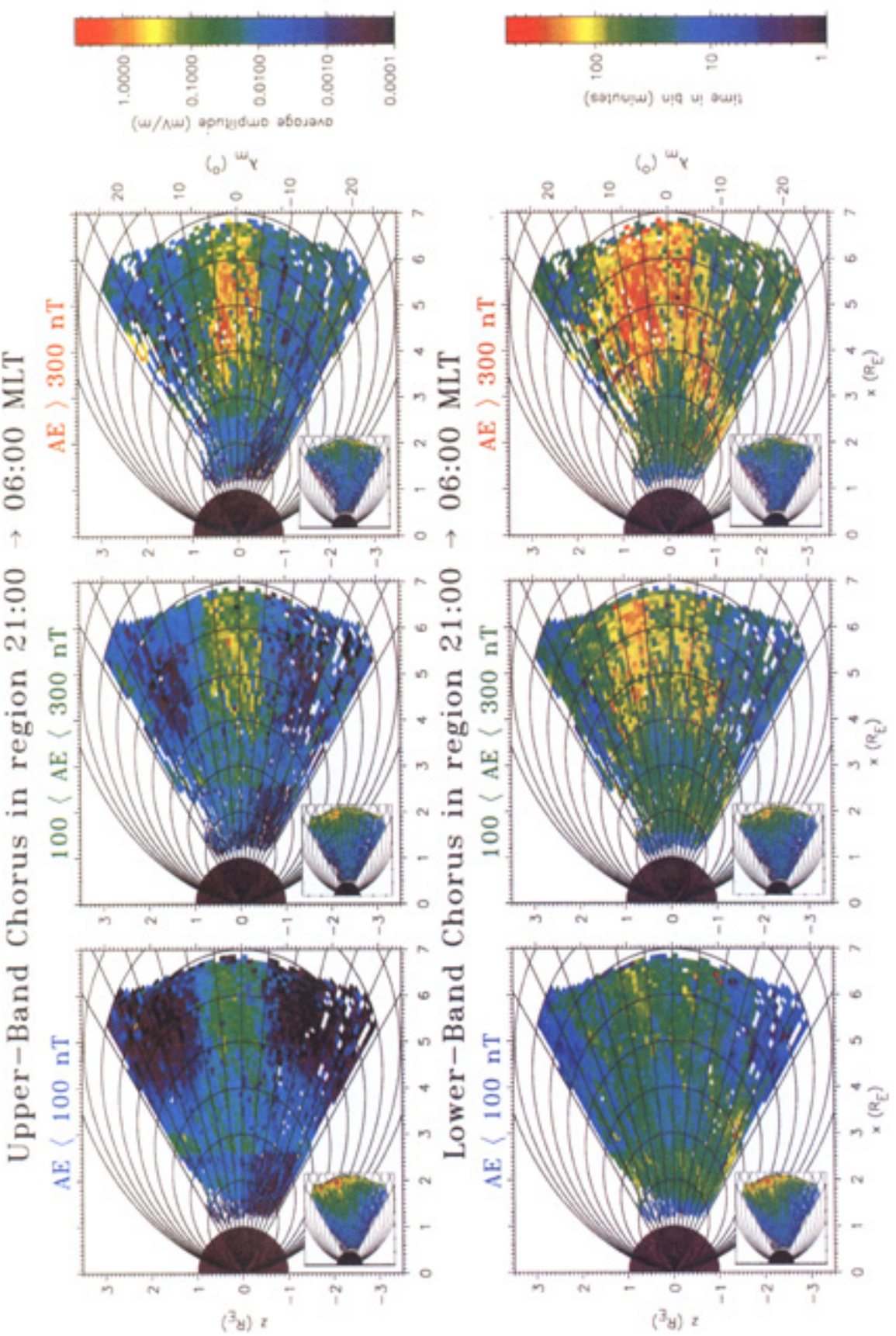

Plate 5. Substorm dependence of the wave amplitudes in the sector 2100-0600 MLT for lower band chorus (lower panels) and upper band chorus (upper panels) as a function of the radial distance from the center of the Earth projected onto the plane of the magnetic equator, x, and GSM z. The average amplitudes are shown in the large panels, together with the corresponding sampling distributions in the small panels.

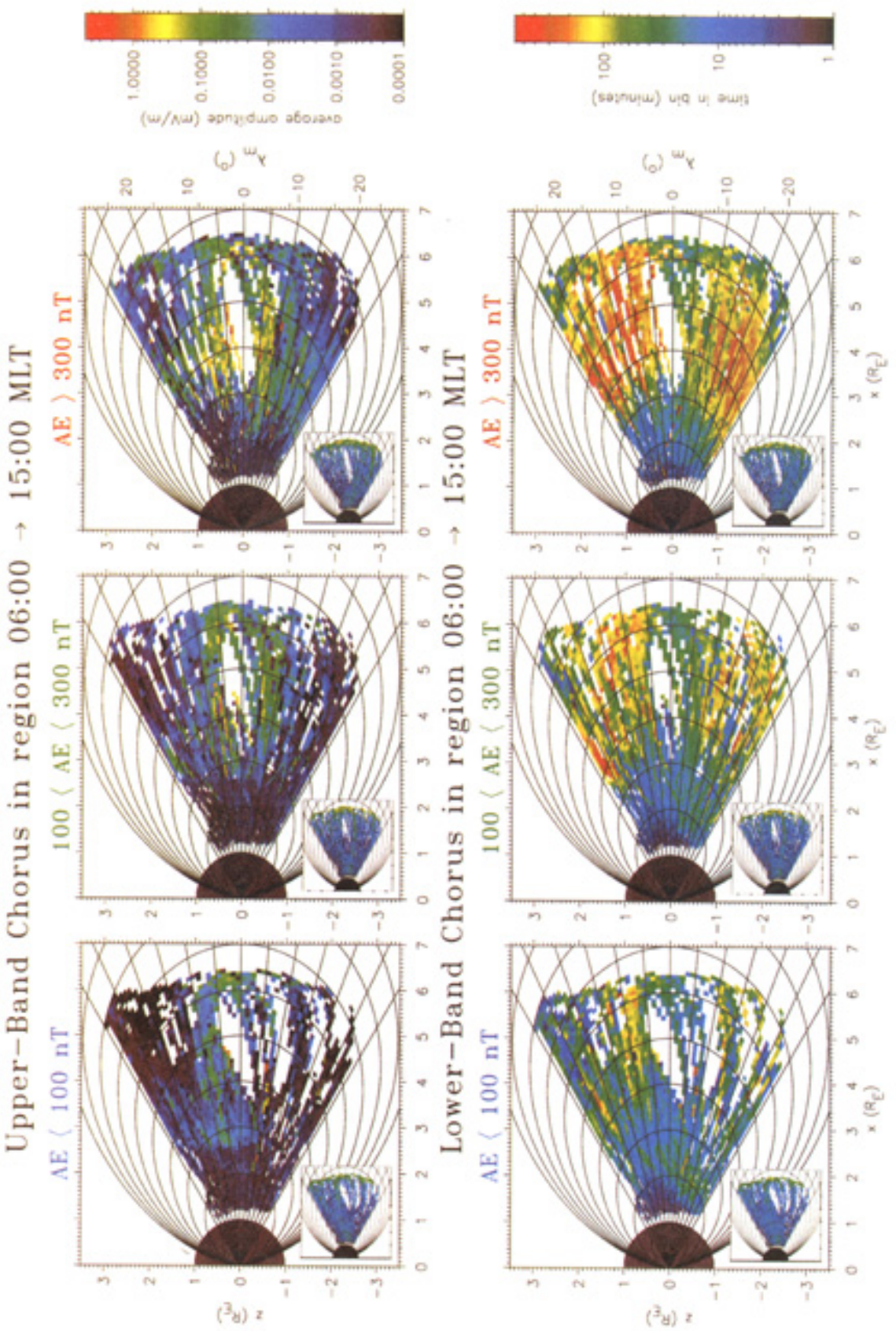

Plate 6. Substorm dependence of the wave amplitudes in the sector 0600-1500 MLT for lower band chorus (lower panels) and upper band chorus (upper panels) as a function of the radial distance from the center of the Earth projected onto the plane of the magnetic equator, x, and GSM z. The average amplitudes are shown in the large panels, together with the corresponding sampling distributions in the small panels.

The outer population of substorm-independent upper band chorus emissions occurs outside the line $x = 2.6\ R_E$ and extend to approximately $L = 5$ during quiet times. These emissions appear stronger in the Northern Hemisphere but can also be seen south of the equator. These signals are due to a combination of lightning-generated whistlers and high-powered navigation transmitters, since $f_{ce}/2 < 25$ kHz in this region.

Signals for which $f < f_{ce}/2$ may be guided by the Earth's magnetic field, and by plasma density gradients. This may explain the symmetry of the lower band emissions about the magnetic equator inside $x = 2.6\ R_E$ where $f_{ce}/2 \geq 25$ kHz. There is evidence for some asymmetry of these emissions in the region 0600-1500 MLT, but this could be due to a sampling effect, since the region south of the equator inside $L = 3$ is sampled largely between 0600 and 1030 MLT, whereas the region above is sampled largely between 1030 and 1500 MLT.

8. Conclusions

The main conclusions from this study can be summarized as follows:

1. Outside $L = 3$ the chorus emissions are largely substorm-dependent and all chorus emissions are enhanced when substorm activity is enhanced. The extent of the emissions is also substorm-dependent, the inner boundary lying outside the plasmapause and moving to smaller L with the plasmapause during active conditions.

2. The equatorial chorus is strongest in the lower band during active conditions with peak amplitudes typically >0.5 mV m^{-1} predominantly in the region $3 < L < 7$, between 2300 and 1300 MLT, consistent with keV electron injection from substorms near midnight and subsequent drift around dawn to the dayside.

3. The high-latitude chorus is strongest in the lower band during active conditions, with peak amplitudes typically >0.5 mV m^{-1} in the region $3 < L < 7$ over a range of local times on the dayside, principally in the range 0600-1500 MLT, consistent with generation in the horns of the magnetosphere.

4. An inner region of weak, substorm-independent emissions is seen largely on the nightside during quiet and moderate conditions. These emissions lie inside the plasmapause and are attributed to signals from lightning and ground-based VLF transmitters.

5. Our results support the theory of electron acceleration by whistler mode chorus. The results suggest that electron acceleration by whistler mode chorus during/following geomagnetic storms can be effective only when there are periods of prolonged substorm activity following the main phase of the geomagnetic storm. Conversely, if the IMF turns strongly northward during the recovery phase, then the wave amplitudes will decay and the electron acceleration by whistler mode chorus should cease. We suggest this as one reason why not all storms result in significant electron acceleration.

6. These results suggest that understanding the relationship between substorms and geomagnetic storms is very important for resolving the electron acceleration problem.

Acknowledgments. We thank the World Data Centre C1 for STP at the Rutherford Appleton Laboratory and the NSSDC Omniweb for providing the geomagnetic indices and solar wind parameters used in this paper. We thank Richard Thorne, Andy Smith, and Roger Iles for many helpful discussions.

Michel Blanc thanks Michel Parrot and Xinlin Li for their assistance in evaluating this paper.

References

Anderson, R. R., CRRES plasma wave observations during quiet time, during geomagnetic disturbances, and during chemical releases, in *Dusty Plasma, Noise and Chaos in Space and in the Laboratory*, edited by H. Kikuchi, p. 73, Plenum, New York, 1994.

Anderson, R. R., D. A. Gurnett, and D. L. Odem, CRRES plasma wave experiment, *J. Spacecr. Rockets, 29*, 570, 1992.

Blake, J. B., D. N. Baker, N. Turner, K. W. Olgilvie, and R. P. Lepping, Correlation of changes in the outer-zone relativistic-electron population with upstream solar wind and magnetic field measurements, *Geophys. Res. Lett., 24*, 927, 1997.

Carpenter, D. L., and R. R. Anderson, An ISEE/whistler model of equatorial electron density in the magnetosphere, *J. Geophys. Res., 97*, 1097, 1992.

Fujimoto, M., and A. Nishida, Energization and anisotropization of energetic electrons in the Earth's radiation belt by the recirculation process, *J. Geophys. Res., 95*, 4265, 1990.

Helliwell, R. H., *Whistlers and Related Ionospheric Phenomena*, Stanford Univ. Press, Stanford, Calif., 1965.

Horne, R. B., and R. M. Thorne, Potential waves for relativistic electron scattering and stochastic acceleration during magnetic storms, *Geophys. Res. Lett., 25*, 3011, 1998.

Hudson, M. K., S. R. Elkington, J. G. Lyon, and C. C. Goodrich, Increase in relativistic electron flux in the inner magnetosphere: ULF wave mode structure, *Adv. Space Res.*, in press, 2000.

Iles, R. H. A., A. N. Fazakerley, A. D. Johnstone, and P. Bühler, The relativistic electron response during magnetic storms, in *Proceedings of the Space Radiation Environment Workshop*, DERA, Farnborough, UK, 2000.

Koons, H. C., and J. L. Roeder, A survey of equatorial magnetospheric wave activity between 5 and 8 R_E, *Planet. Space Sci., 38,* 1335, 1990.

Li, X., D. N. Baker, M. Temerin, T. E. Cayton, G. D. Reeves, R. A. Christiansen, J. B. Blake, M. D. Looper, R. Nakamura, and S. G. Kanekal, Multisatellite observations of the outer zone electron variation during the November 3-4, 1993, magnetic storm, *J. Geophys. Res., 102*, 14,123, 1997a.

Li, X., D. N. Baker, M. Temerin, D. Larson, R. P. Lin, G. D. Reeves, M. Looper, S. G. Kanekal, and R. A. Mewaldt, Are energetic electrons in the solar wind the source of the outer radiation belt?, *Geophys. Res. Lett., 24*, 923, 1997b.

Liu, W. W., G. Rostoker, and D. N. Baker, Internal acceleration of relativistic electrons by large-amplitude ULF pulsations, *J. Geophys. Res., 104*, 17,391, 1999.

Lyons, L. R., R. M. Thorne, and C. F. Kennel, Pitch angle

diffusion of radiation belt electrons within the plasmasphere, *J. Geophys. Res., 77*, 3455, 1972.

Maeda, K., P. H. Smith, and R. R. Anderson, VLF emissions from ring current electrons, *Nature, 263*, 5572, 1976.

Meredith, N. P., R. B. Horne, A. D. Johnstone, and R. R. Anderson, The temporal evolution of electron distributions and associated wave activity following substorm injections in the inner magnetosphere, *J. Geophys. Res., 105*, 12,907, 2000.

Parrot, M., and C. A. Gaye, A statistical survey of ELF waves in a geostationary orbit, *Geophys. Res. Lett., 21*, 2463, 1994.

Reeves, G. D., Relativistic electrons and magnetic storms: 1992-1995, *Geophys. Res. Lett., 25*, 1817, 1998.

Rostoker, G., S. Skone, and D. N. Baker, On the origin of relativistic electrons in the magnetosphere associated with some geomagnetic storms, *Geophys. Res. Lett., 25*, 3701, 1998.

Schulz, M., and L. Lanzerotti, Particle diffusion in the radiation belts, Springer-Verlag, New York, 1974.

Sheldon, R. B., H. E. Spence, J. D. Sullivan, T. A. Fritz, and J. Chen, The discovery of trapped energetic electrons in the outer cusp, *Geophys. Res. Lett., 25*, 1825, 1998.

Singer, H. J., W. P. Sullivan, P. Anderson, F. Mozer, P. Harvey, J. Wygant, and W. McNeil, Fluxgate magnetometer instrument on the CRRES, *J. Spacecr. Rockets, 29*, 599, 1992.

Smith, A. J., and P. J. Jenkins, A survey of natural electromagnetic noise in the frequency range f= 1-10 kHz at Halley station Antarctica, 1, Radio atmospherics from lightning, *J. Atmos. and Sol. Terr. Phys., 60*, 263, 1998.

Summers, D., and C. Ma, A model for generating relativistic electrons in the Earth's inner magnetosphere based on gyroresonant wave-particle interactions, *J. Geophys. Res., 105*, 2625, 2000.

Summers, D., R. M. Thorne, and F. Xiaio, Relativistic theory of wave-particle resonant diffusion with application to electron acceleration in the magnetosphere, *J. Geophys. Res., 103*, 20,487, 1998.

Thorne, R. M., and R. B. Horne, Landau damping of magnetospherically reflected whistlers, *J. Geophys. Res., 99*, 17,249, 1994.

Thorne, R. M., and C. F. Kennel, Relativistic electron precipitation during magnetic storm main phase, *J. Geophys. Res., 76*, 4446, 1971.

Tsurutani, B. T., and E. J. Smith, Postmidnight chorus: A substorm phenomenon, *J. Geophys. Res., 79*, 118, 1974.

Tsurutani, B. T., and E. J. Smith, Two types of magnetospheric ELF chorus and their substorm dependencies, *J. Geophys. Res., 82*, 5112, 1977.

Vampola, A. L., J. V. Osborn, and B. M. Johnson, CRRES magnetic electron spectrometer, *J. Spacecr. Rockets, 29*, 592, 1992.

R. R. Anderson, Department of Physics and Astronomy, University of Iowa, Iowa City, IA 52242-1479. (roger-r-anderson@uiowa.edu)

R. B. Horne, British Antarctic Survey, Natural Environment Research Council, Madingley Road, Cambridge, CB3 0ET, England, UK. (r.horne@bas.ac.uk)

N. P. Meredith, Mullard Space Science Laboratory, University College London, Holmbury St. Mary, Dorking, Surrey, RH5 6NT, England, UK. (npm@mssl.ucl.ac.uk)

(Received August 28, 2000; revised October 20, 2000; accepted November 4, 2000.)